Atomization and Mixing Characteristics of an Unlike-Doublet Impinging-Jet Spray

W.H. Lai, W. Huang, and C.J. Chu
Department of Aeronautics and Astronautics
National Cheng Kung University
Tainan, Taiwan, 701, R.O.C.
Tel:(886)6-2757575ext.63694, Fax:(886)6-2389940
E-mail:whlai@mail.ncku.edu.tw

Abstract

The spray characteristics of an unlike-doublet impinging-jet are investigated in this work. The working fluids are purified water and 95% alcohol-water solution. Impingement angle is selected 60^o. The injector is made of stainless steel with orifice diameter of 0.5 mm. Results show that spray patterns of the unlike-doublet impinging-jet are quite similar with those of like-doublet, despite of the difference in physical properties of these two impinging jets. Mean drop size, measured by using light diffraction particle sizer, has a peak value along the axis through the impingement point. An asymptotic value of 50 μm in drop size is approached when jet velocity is elevated high enough, that is the same with the like-doublet impinging-jet. The variation of deviation angle with jets momentum ratio is quite matching with the theoretical derivation. Results of mixture ratio analysis show that jets will penetrate each other through the impingement point.

Introduction

To take the advantages of spontaneous reaction of fuel and oxidizer, hypergolic propellants was widely utilized in the small bipropellant liquid rocket to play the roles of attitude control and orbit transit of space flight vehicles. However, the device which can obtain an optimum atomization, mixing and combustion of propellants to reduce the length as well as weight of combustor and to enhance the combustion efficiency is the major concern in the design of the injector. Impinging-jet injector, with its simplicity in geometry, easy for manufacture and maintenance, instantaneously atomization and mixing of propellants, is usually adopted to act the atomization, mixing, combustion in the small bipropellant liquid rocket engine.

Impinging-jet injector utilizes the impact of two or more liquid jets to disintegrate the liquid into ligament and small drops to accomplish the atomization and mixing in the same time. In order to enhance the combustion efficiency in the rocket, characteristics of impinging jets should be clearly understood. Many authors had attacked this territory in the past decades. Unfortunately, clear information is still lacking, especially for the unlike impinging jets, and it deserves further studies. The present work is concentrated on the flow pattern, atomization and mixing characteristics of an unlike-doublet impinging-jet injector. These results should be of critical importance as the basis of rocket engine design.

Base on the observation of like-doublet impinging-jet made of two 70% glycerol solution jets in the impingement angle of 90^{o}, Heidmann *et al*. [1] identify the flow patterns of impinging jets as (a)closed-rim, (b)periodic-drop, (c)open-rim, and (d)fully developed with increasing jets velocities. Resent study by Lai *et al*. [2], by changing liquid properties of viscosity and surface tension, the flow of the impinging jets are further identified as ten different patterns. They are (a)closed-rim cascade, (b)closed-rim without drop shedding, (c) closed-rim with periodic drop, (d)closed-rim with drop shedding, (e)closed-rim with perforated film, (f)open-rim without drop shedding, (g)open-rim with drop shedding, (h)open-rim with perforated film, (i) open-rim with both drop-shedding and perforated, (j)fully developed. Lai and Wang [3], in their study, the development of flow patterns with jets velocity was shown deeply affected by varying viscosity of working fluid. To investigate the spray characteristics of an impinging-jet injector, Huang [4] found that, under lower jets velocity regions, mean drop diameter (SMD) formed by impinging jets increases with increasing viscosity and surface tension of working fluid. However, the effect of fluid properties on mean drop size diminishes once jets velocity over a certain value. And all of the mean drop size approach 50μm in diameter.

Vassallo *et al*. [5] studied the characteristics of impinging two and four water jets. His results show that, with increasing Reynolds number, volume flux of spray formed decreases in the center, increases in the direction parallel to the plane of jets, and remain approximately constant along the direction parallel to the plane of liquid sheet. Besides, droplet diameter decreases and number density increases with increasing jets flow rate. Rupe [6], using carbon tetrachloride and water as simulants to study the mixing behavior of a pair of jets-impingement at jet velocity of around 30 m/sec. Results show that mass distribution significantly changes with momentum ratio of the jets. However, local mixture ratio along the major axis of the spray cross-section is nearly constant. Meanwhile, the optimum mixture ratio occurred when the momentum of the two jets come into balance.

$$\left(r_1 V_1^2 A_1\right)/\left(r_2 V_2^2 A_2\right) = 1 \tag{1}$$

Riebling [7] studies the mixing of water and n-hexane jets impingement by changing length to diameter ratio (L/d) of injector orifice and the distance of impingement. Ashgriz *et al*. [8], colorizing the working fluid to investigate the mixing of miscible and immiscible impinging jets. Results reveal that two distinct processes, preatomization and postatomization, control the mixing characteristics. The former can be further divided into reflect and transmitive mode. On the other hands, the latter is caused by turbulent dispersion in the spray region.

Other observations include Won [9] and Lee [10], by using the immiscible and miscible fluids to study the effect of momentum ratio variation, symmetric and asymmetric impingement angle on the mixing of an unlike impinging-jet.

Facilities and Instrumentation

The experimental facilities in the present study are designed and set up to accomplish both qualitative and quantitative analysis on the characteristics of the unlike-doublet impinging-jet spray. The setup is schematically demonstrated in Fig. 1. Injectors in the present work are made of stainless steel. The orifice is a straight hole with diameter (d_o) of 0.5 mm and length (L) of 5 mm. In order to diminish the occurrence of instability caused by wall roughness, the orifice are carefully drilled and well polished during manufacturing.

The impinging angle (2θ) is selected as 60^o, and length before impingement is set as 10 mm, schematic illustration of the impinging-jet is shown in Fig.2. The two working fluids are purified water (fluid1) and 95% alcohol-water solution (fluid2). Properties of the working fluids are listed in Table 1. Working fluids are stored in tanks and fed to injectors by high pressure gases. Mass flow rate of the working fluid is controlled by s set of metering valves and is measured by a carefully calibrated turbine flowmeter.

A single exposure camera (Nikon FM2) with a micro lens is used for the observation of the jet-impinging spray patterns. In order to frozen the instantaneous behavior of the impinging-jet, a stroboscope with approximately 400 ns exposure is used as the backward lighting luminance. Sauter mean diameter of the disintegrated drops is measured by a laser diffraction sizing device (INSITEC ensemble particle concentration and size), which is a commercially available and one of the most effective and reliable method for particle measurement in the current state. A patternator with 5X7 sampling matrix, shown in Fig.3, is applied to collect and analyze the mixture ratio distribution of the unlike-doublet impinging-jet spray. Although it is cumbersome, it is still one of the state of the art of the sampling method.

Results and Discussions

After a series of detail observations and measurements, results of flow patterns, mean drop size, relation between deviation angle of liquid film and momentum ratio, and spatial distribution of mixture ratio of the unlike-doublet impinging jets are presented and discussed in the following paragraphs.

Frozen images of the unlike impinging jets with jet velocities are demonstrated in Figures 4(a-f). It is noted that these two jets are adjusted in equal momentum. Results show that the flow patterns of unlike-doublet impinging-jet are quite similar to that of like-doublet impinging-jet.

At lower jet speed (Fig.4a), jets impinge each other and merge into a single stream at the moment of impingement, and then this merged stream finally breakup into large drops. With increasing jet velocity (Fig.4b), a small film formed by jets impingement. Drops periodically disintegrate from the rim enclosed the liquid film, and then coalesce to form larger drops. With jets velocity further increased (Fig.4c), the closed-rim pattern forms. It is worth to note that an erratic rim is observed. This can be resorted to the unbalance in properties of the two liquid and therefore induce vibration and disturbance in the rim. Liquids flow down along the rim and merge at the lower tip of the film and then breakup into drops. This phenomenon has never been observed in like-doublet impinging jets. Further increasing jets velocity to high enough (Fig.4d), the fully-developed pattern forms. This is quite the same with the like-doublet impingement. Circular ligaments radially disintegrate from the impinging point and subsequently breakup into small drops. The ligament and drops get much smaller with increasing jets velocity in the fully-developed regime (Fig.4e).

Drop size measurements are conducted at 68 mm beneath the impingement point, and along the direction parallel to the plane of liquid film (lateral direction). Results of mean drop size (D_{32}) distribution are shown in Fig.5. It reveals that mean drop size is greater toward the central line regime of impingement point and a peak formed at the center. This trend of size distribution can be attributed to major concentrating of liquid near the center line regime and, therefore, larger drops and ligaments formed after impingement. It also shows that the peak distribution becomes much more protruding at lower jet velocities. It can be resorted to the less energy provided for jet breakup at lower jet velocity, which makes it difficult to disintegrate liquid into small drops. On the other hand, it also shows that mean drop size get smaller and the distribution becomes flatten with increasing jet velocities. However, increasing jets velocity up to over 20 m/sec, mean drop size becomes much smaller and gradually approaches an asymptotic value of about 50 μm (Fig.6). This asymptotic value is directly dependent upon jet diameter and is independent on the working fluids [4].

For an unlike-doublet impinging-jet spray, the resulting spray will deviate from the symmetric axis of the two jets if the two jets are not of the same momentum. In this study, jet velocity of fluid2 (V_{j2}) is set as 6, 9,12, and 15 m/sec, and adjust jet velocity of fluid1 (V_{j1}) to change the mass flow ratio and momentum ratio as well. Long duration exposure photographs are taken for the deviation analysis. According to theoretical derivation, deviation angle δ can be expressed as

$$d = \tan^{-1}\left[\frac{m_1 V_{j1}\sin q_1 - m_2 V_{j2}\sin q_2}{m_1 V_{j1}\cos q_1 + m_2 V_{j2}\cos q_2}\right]. \quad (2)$$

And for a symmetric jets impingement, $q_1 = q_2 = q/2 = 30^{o}$ in this experiment.

Results of deviation angle measurement are demonstrated in Fig.7. On the other hands, Fig.8 shows the comparison between theoretical derivation and the measured data. In Fig.7, jet velocity of fluid2 ($V_{j,2}$) is set as 6, 9, 12, and 15 m/sec respectively. Deviation angle is observed by changing velocity of fluid1 ($V_{j,1}$) to make differences in momentum ratio. Results show that the variation of deviation angle is almost the same for all jets velocity, and quite compliant with the conservation of momentum. It also shows, from Fig.8, the measured data match very well with the theoretically derived data, especially for $V_{j,2}$ of 6 and 9 m/sec. The measured data deviate for $V_{j,2}$ of 12 and 15 m/sec. This can be attributed to the spray dispensing wider for increasing jets velocity. Which makes it difficult to clearly define the deviation angle, and therefore error of measurement generated.

Collecting the atomized drops by the patternator at 100 and 150 mm at downstream of the impingement point, the mixture ratio distribution of the unlike-doublet impinging-jet are analyzed and presented in Fig.9. From the results, Figs.9a and 9b show that the atomized liquid with larger density toward the $V_{j,2}$ end, and decreases toward the $V_{j,1}$ end, along the direction of plane formed by the two jets. This trend is caused by the penetrating of fluids through the point of impingement, the same with the results of transmitive mode presented by Asghriz [8]. Changing the jets velocity to verity the tendency of mixture ratio distribution varying with jet velocity, Figure10 shows the tendency is always the same for all jets velocities. On the other hands, Figure11 shows that mixture ratio distribution is less relevant to sampling position beneath the impingement point and jet velocity, provided that the momentum ratio remains the same.

Conclusions

After a series of detail observation on the unlike-doublet impinging-jet, conclusions are drawn as follow,

1. The spray patterns of the unlike-doublet impinging-jet are quite the same with that of like-doublet, even there are differences in physical properties of the two impinging jets.
2. Mean drop size of the unlike-doublet impinging-jet will form a peak value along the axis through the impingement point. And drop size get smaller for increasing jets velocity. An asymptotic value of 50 μm in drop size is approached, that is the same with the like-doublet impinging-jet.
3. The variation of deviation angle with jets momentum ratio is quite matching with the theoretical derivation.
4. Results of mixture ratio show that jets will penetrate through each other at point of impingement. This is also agree with the transmitive mode presented by Asghriz [8].

Acknowledgement

This work was supported by the National Science Council, Taiwan, the Republic of China, under contract No. NSC 86-2212-006-060.

References

[1] Heidmann, M.F., Priem, R.J., Humphrey, J.C., NACA TN-3835, 1957.

[2] Lai, W.H., Huang, W., Huang, T.H., Jiang, T.L., The Second Asia-Pacific Conference On Combustion, Tainan, Taiwan, May 9-12, 1999.

[3] Lai, W.H., Wang, H.C., *AIAA 2002-3700, 38th AIAA/ASME/SAE/ASEE Joint Propulsion Conference and Exhibit*, Indianapolis, Indiana, 7-10 July, 2002.

[4] Huang, W., *Ph.D. Thesis*, Institute of Aeronautics and Astronautics, National Cheng Kung University, Tainan, Taiwan, R.O.C., Jung, 1998.

[5] Vassallo, P., Ashgriz, N., and Boorady, F.A., *Journal of Propulsion and Power*, vol. 8, No. 5, pp. 980-986, 1992.

[6] Rupe, J.H., *JPL Prog*. Rep.20-195,1956.

[7] Riebling, R.W., "Effect of Orifice Length-to- Diameter Ratio on Mixing in The Spray From a Pair of Unlike Impinging Jets," *Journal of Spacecraft*, vol. 7, No. 7, 1970, pp. 894-896.

[8] Ashgriz, N., Brocklehurst, W., and Talley, D.G., *Journal of Propulsion and Power*, vol. 17, No. 3, 2001.

[9] Won, Y.D., Cho, Y.H., Lee, S.W., Yoon, W.S., *Journal of Propulsion and Power*, vol. 18, No. 4, 2002.

[10] Lee, C.H., Jung, Y.H., and Chung, S.H., *Atomization and Spray*, vol. 9, 1999, pp. 193-213.

Table 1 Properties of the working fluids.

Item	Density, r (Kg/m^3)	Viscosity, $m \times 10^{-3}$(Ns/m^2)	Surface Tension, $s \times 10^{-3}$ (N/m)
Fluid1	1.0	1.0	74.5
Fluid2	0.803	1.0	22.26

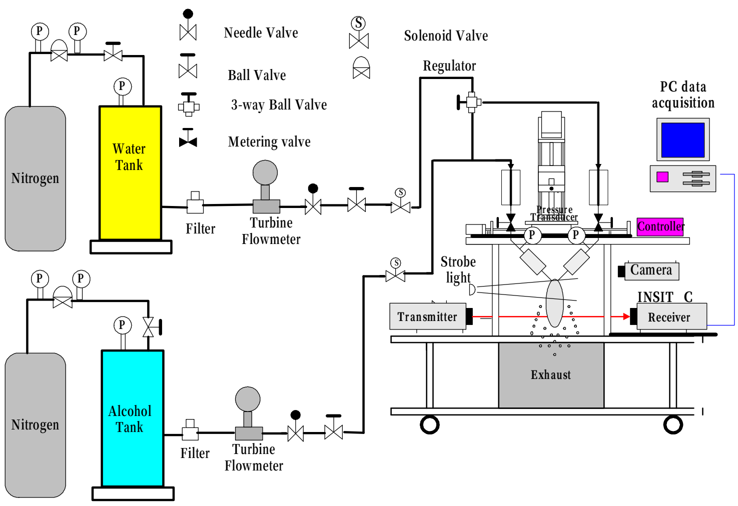

Fig.1 Experimental facilities.

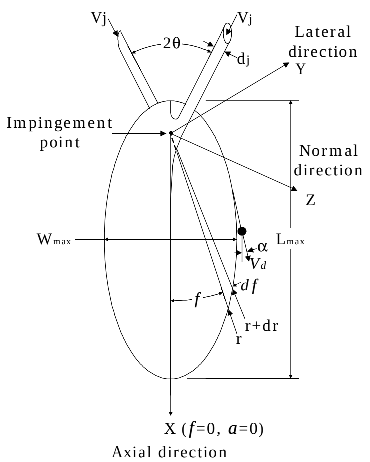

Fig.2 Schematic illustration of the impinging-jet.

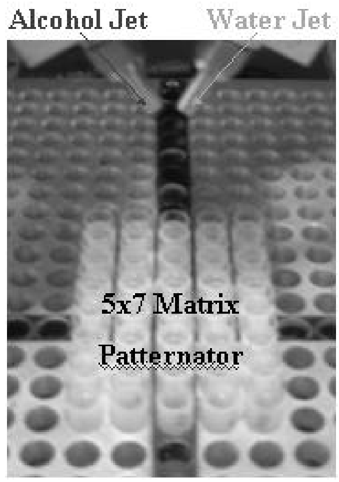

Fig.3 Patternator

a)	(b)	(c)	(d)	(e)
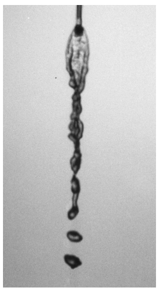	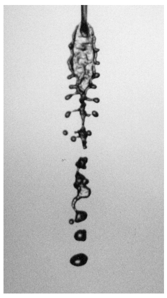	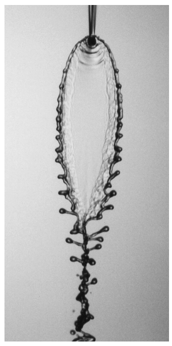	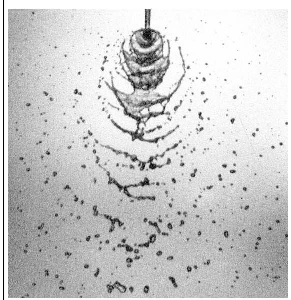	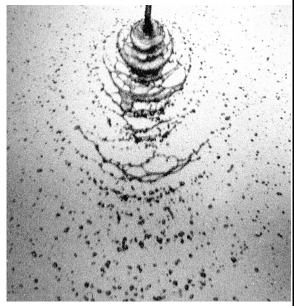
$V_{j,1}$ = 1.6m/sec	$V_{j,1}$ = 2.0m/sec	$V_{j,1}$ = 3.8m/sec	$V_{j,1}$ = 5.1m/sec	$V_{j,1}$ = 6.9m/sec

Fig.4 Flow patterns of the unlike-doublet impinging jets with identical momentum.

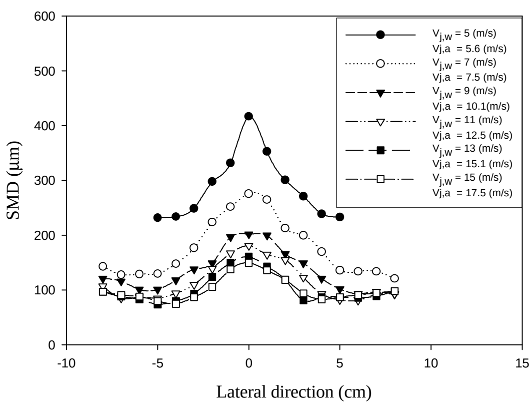

Fig.5 Size distribution in lateral direction.

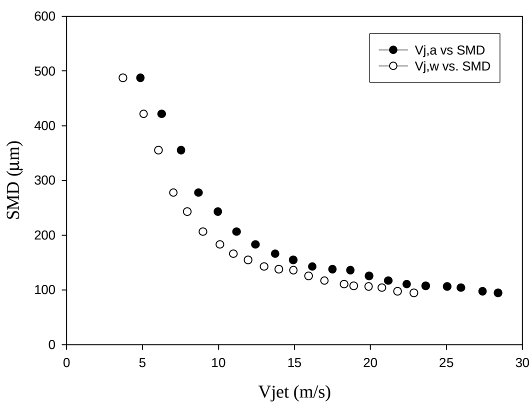

Fig.6 Size variation with jet velocities.

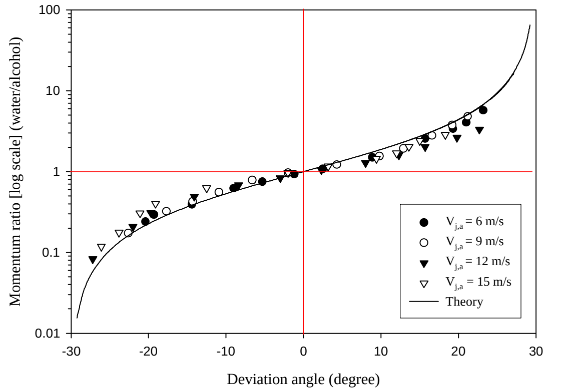

Fig.7 Variation of deviation angle with jet's momentum ratio.

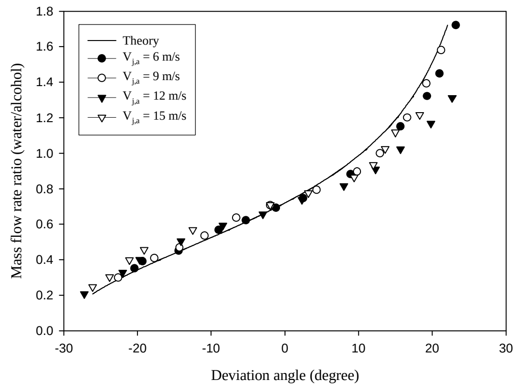

Fig.8 Comparison of measured deviation angle with theoretical predicted.

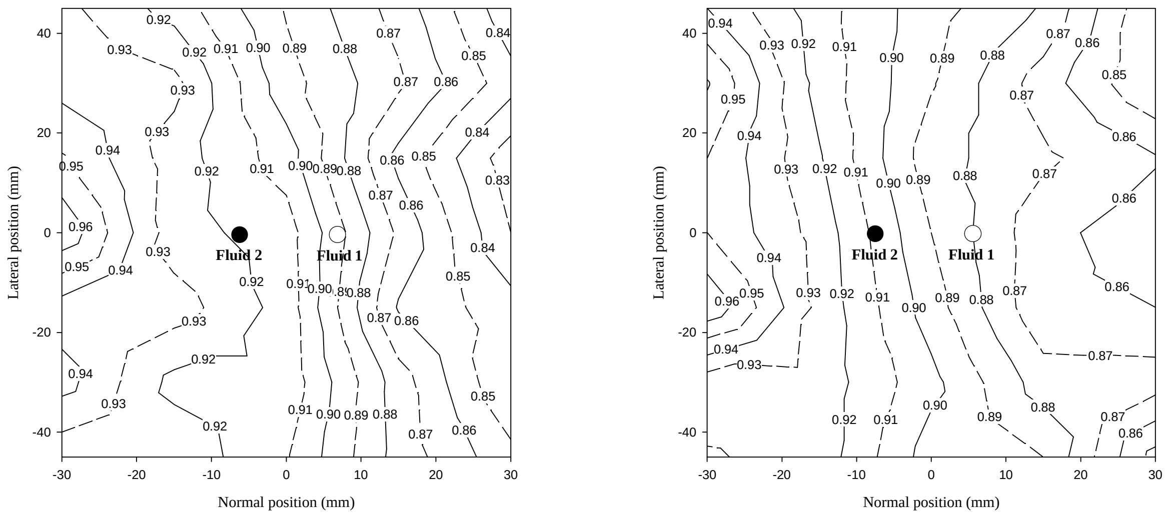

(a) 100mm (b) 150mm

Fig.9 Mixture ratio distribution contour at downstream of the impingement point.

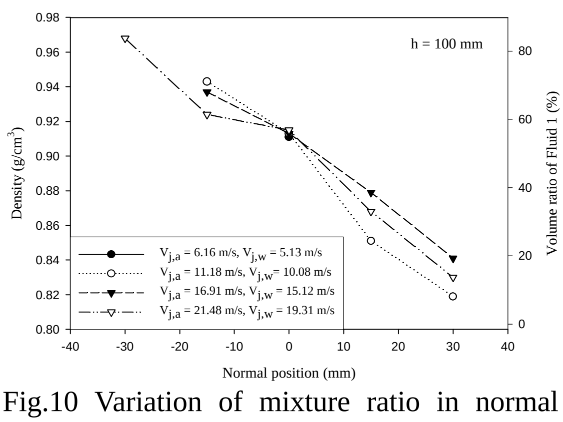

Fig.10 Variation of mixture ratio in normal direction (perpendicular to the liquid film).

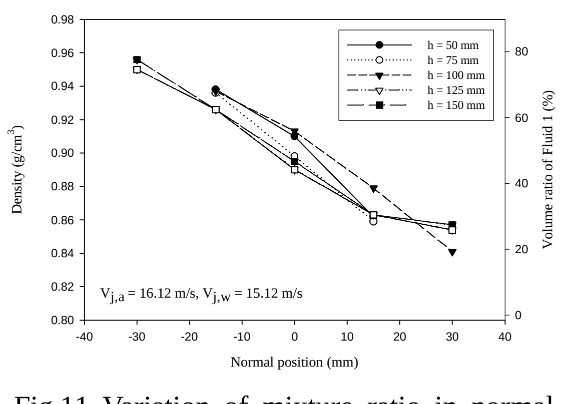

Fig.11 Variation of mixture ratio in normal direction along downstream.